

A Transcriptomic study of probenecid on injured spinal cords in mice

Yu-Xin Zhang^{Equal first author, 1, 2, 3}, Sai-Nan Wang^{Equal first author, 1, 2}, Jing Chen^{1, 2}, Jian-Guo Hu^{Corresp., 1, 2}, He-Zuo Lü^{Corresp. 1, 2}

¹ Clinical Laboratory, the First Affiliated Hospital of Bengbu Medical College, Bengbu, China

² Anhui Key Laboratory of Tissue Transplantation, the First Affiliated Hospital of Bengbu Medical College, Bengbu, China

³ Department of Biochemistry and Molecular Biology, Bengbu Medical College, Bengbu, China

Corresponding Authors: Jian-Guo Hu, He-Zuo Lü

Email address: jghu9200@163.com, lhz233003@163.com

Background. Recent studies have found that probenecid has neuroprotective and reparative effects on central nervous system (CNS) injuries. However, its effect on genome-wide transcription in acute spinal cord injury (SCI) remains unknown. In the present study, RNA sequencing (RNA-Seq) is used to analyze the effect of probenecid on the local expression of gene transcription eight hours after spinal injury. **Methods.** An Infinite Horizon impactor was used to perform contusive SCI in mice. The SCI model was made by using a rod (1.3 mm diameter) with a force of 50 Kdynes. Sham-operated mice only received a laminectomy without contusive injury. The injured mice were randomly assigned into either the control (SCI_C) or probenecid injection (SCI_P) group. In the latter group, the probenecid drug was intraperitoneally injected (0.5mg/kg) immediately following injury. Eight hours after the injury or laminectomy, the spinal cords were removed from the mice in both groups. The total RNAs were extracted and purified for library preparation and transcriptome sequencing. Differential gene expressions (DEGs) of the three groups — sham, SCI_C and SCI_P — were analyzed using a DESeq software. Gene Ontology (GO) and Kyoto Encyclopedia of Genes and Genomes (KEGG) enrichment analysis of DEGs were performed using a GOseq R package and KOBAS software. Real-time quantitative reverse-transcriptase polymerase chain reaction (RT-qPCR) was used to validate RNA-Seq results. **Results.** RNA-Seq showed that, compared to the SCI_C group, the number of DEGs was 641 in the SCI_P group (286 upregulated and 355 downregulated). According to GO analysis, DEGs were most enriched in extracellular matrix, collagen trimer, protein bounding and sequence specific DNA binding. KEGG analysis showed that the most enriched pathways included: cell adhesion molecules (CAMs), Leukocyte transendothelial migration, ECM-receptor interactions, PI3K-Akt signaling pathways, hematopoietic cell lineages, focal adhesions, the Rap1 signaling pathway, etc. The sequence data have been deposited into a Sequence Read Archive

(<https://www.ncbi.nlm.nih.gov/sra/PRJNA554464>).

1 **A Transcriptomic study of probenecid on injured**
2 **spinal cords in mice**

3

4 Yu-Xin Zhang^{1,2,3&}, Sai-Nan Wang^{1,2&}, Jing Chen^{1,2}, Jian-Guo Hu^{1,2*}, He-Zuo Lü^{1,2*}

5

6 ¹ Clinical Laboratory, the First Affiliated Hospital of Bengbu Medical College, Anhui 233004,
7 P.R. China

8 ²Anhui Key Laboratory of Tissue Transplantation, the First Affiliated Hospital of Bengbu
9 Medical College, Anhui 233004, P.R. China

10 ³Department of Biochemistry and Molecular Biology, Bengbu Medical College, Anhui 233030,
11 P.R. China

12

13 & These authors contributed equally to this work

14

15 * Co-corresponding authors:

16 Jian-Guo Hu

17 Email address: jghu9200@163.com

18 He-Zuo Lü

19 Email address: lhz233003@163.com

20

21 Please address correspondence to:

22 He-Zuo Lü, M.D. Ph.D., Professor

23 Anhui Key Laboratory of Tissue Transplantation

24 the First Affiliated Hospital of Bengbu Medical College

25 287 Chang Huai Road

26 Bengbu 233004, P.R. China

27 Tel: +86-552-3170692

28 E-mail: lhz233003@163.com

29

30

31

32

33

34 **Abstract**

35

36 **Background.** Recent studies have found that probenecid has neuroprotective and reparative
37 effects on central nervous system (CNS) injuries. However, its effect on genome-wide
38 transcription in acute spinal cord injury (SCI) remains unknown. In the present study, RNA
39 sequencing (RNA-Seq) is used to analyze the effect of probenecid on the local expression of
40 gene transcription eight hours after spinal injury.

41 **Methods.** An Infinite Horizon impactor was used to perform contusive SCI in mice. The SCI
42 model was made by using a rod (1.3 mm diameter) with a force of 50 Kdynes. Sham-operated
43 mice only received a laminectomy without contusive injury. The injured mice were randomly
44 assigned into either the control (SCI_C) or probenecid injection (SCI_P) group. In the latter
45 group, the probenecid drug was intraperitoneally injected (0.5mg/kg) immediately following
46 injury. Eight hours after the injury or laminectomy, the spinal cords were removed from the mice
47 in both groups. The total RNAs were extracted and purified for library preparation and
48 transcriptome sequencing. Differential gene expressions (DEGs) of the three groups — sham,
49 SCI_C and SCI_P — were analyzed using a DESeq software. Gene Ontology (GO) and Kyoto
50 Encyclopedia of Genes and Genomes (KEGG) enrichment analysis of DEGs were performed
51 using a GSeq R package and KOBAS software. Real-time quantitative reverse-transcriptase
52 polymerase chain reaction (RT-qPCR) was used to validate RNA-Seq results.

53 **Results.** RNA-Seq showed that, compared to the SCI_C group, the number of DEGs was 641 in
54 the SCI_P group (286 upregulated and 355 downregulated). According to GO analysis, DEGs
55 were most enriched in extracellular matrix, collagen trimer, protein bounding and sequence
56 specific DNA binding. KEGG analysis showed that the most enriched pathways included: cell
57 adhesion molecules (CAMs), Leukocyte transendothelial migration, ECM-receptor interactions,

58 PI3K-Akt signaling pathways, hematopoietic cell lineages, focal adhesions, the Rap1 signaling
59 pathway, etc. The sequence data have been deposited into a Sequence Read Archive
60 (<https://www.ncbi.nlm.nih.gov/sra/PRJNA554464>).

61

62 **Introduction**

63 The term spinal cord injury (SCI) refers to a variety of injuries to the spinal cord. According to
64 the severity of injury the symptoms may vary, ranging from pain to a complete loss of movement
65 and sensory function. SCI affects millions of people worldwide, typically for life (Friedli et al.
66 2015). In the United States, there are around 12,000 to 20,000 new SCI cases a year, with more
67 than 280,000 patients confined to wheelchairs (Singh et al. 2014). In the past decade, the SCI
68 cases in China have risen tenfold, and are now increasing by about 60,000 cases every year (Qiu
69 2009). SCI has a high rate of disability and mortality, which creates a heavy burden for patients,
70 their families and society (Krueger et al. 2013). Therefore, it is imperative to explore effective
71 treatment methods for repairing SCI in order to improve the quality of life of patients and reduce
72 the burden of social medical care.

73 Pathological processes following traumatic SCI can be characterized as primary and secondary
74 injuries (Geisler et al. 2002; McDonald & Sadowsky 2002). Primary injury refers to the direct
75 injury of the spinal cord by mechanical force, including compression, contusion, laceration and
76 penetration. Secondary injury refers to edema, ischemia, local inflammation and electrolyte
77 changes. These changes can cause an accumulation of lipid peroxides and oxygen-free radicals,
78 as well as a release of inflammatory factors and proteases. This can ultimately lead to a large
79 amount of cell apoptosis or necrosis, which further aggravates the damage to the neurons and
80 axons (Ahuja et al. 2017; Oyinbo 2011; Tran et al. 2018).

81 Probenecid is an organic anion-transport protein inhibitor, which has been widely used in clinical
82 settings (Hagos et al. 2017; Tollner et al. 2015). For example, probenecid has been used as a
83 synergist in the treatment of gout and antibiotics (Baranova et al. 2004; Papadopoulos &
84 Verkman 2008). It can reduce the degree of cognitive impairment in afflicted rats (Mawhinney et
85 al. 2011), as well as reverse cerebral ischemic injury and cellular inflammation (Wei et al. 2015;
86 Xiong et al. 2014). The combination of probenecid and N-Acetylcysteine could potentially both
87 maintain intracellular GSH concentrations and inhibit neuronal death after a traumatic stretch
88 injury (Du et al. 2016). Some studies report that probenecid can also reduce neuropathic pain in
89 the spinal cord (Bravo et al. 2014; Pineda-Farias et al. 2013). Therefore, these reports indicate
90 that probenecid has neuroprotective and reparative effects on central nervous system (CNS)
91 injuries. However, whether the drug can play a role in treating SCI and whether it can affect the
92 gene expression profiles in injured spinal cords remain unknown. To test this, probenecid was
93 injected intraperitoneally into spinal cord-injured mice immediately after injury. Eight hours
94 after the injury or laminectomy, the spinal cords were removed and RNA-Seq was used to
95 analyze the changes in transcriptome expression in the injured area. Then, the key molecules and
96 signal pathways were screened and identified, providing a new theoretical and experimental
97 basis for SCI clinical treatment.

98

99 **Materials & Methods**

100 **Animals**

101 A total of 27 healthy, clean C57BL/6 female mice (18-20g, 8 weeks old) were used to model
102 SCI. The Animal Care and Use Committee of Bengbu Medical College provided full approval
103 for this research (037/2017). Animal care following surgery was carried out in compliance with

104 the regulations for the management of experimental animals (revised by the Ministry of Science
105 and Technology of China in June 2004), as well as the guidelines and policies on rodent survival
106 surgery provided by the Animal Care and Use Committee of Bengbu Medical College.

107 **Contusive SCI and drug injection**

108 An Infinite Horizon impactor (Precision Systems & Instrumentation, Lexington, KY) was used
109 to perform contusive SCI on the mice. These mice were first anesthetized with 50 mg/kg
110 pentobarbital, followed by the excision of the T9 lamina. A SCI model of this procedure was
111 created using a rod (1.3 mm diameter) with a force of 50 Kdynes. Sham-operated (sham) mice
112 only received a laminectomy without contusive injury.

113 The spinal cord-injured mice were randomly assigned to the solvent control (SCI_C) or
114 probenecid injection (SCI_P) group. The solvent or probenecid (0.5mg/kg) was intraperitoneally
115 injected immediately following injury. The solution (pH 7.3) was prepared as previously
116 described (Hainz et al. 2017).

117 **RNA isolation, quantification and qualification**

118 Eight hours after the injury or laminectomy, the mice were anesthetized and perfused with 10 ml
119 PBS. Their spinal cords (0.5 cm including the injury center) were then removed. The total RNAs
120 from their spinal cords were extracted and purified as previously described (Shi et al. 2017).

121 **Library preparation and transcriptome sequencing**

122 The sequencing libraries were produced by using a NEBNext[®] Ultra[™] RNA Library Prep Kit for
123 Illumina[®] (NEB, USA) as previously described (Shi et al. 2017). Finally, the 125 bp/150 bp
124 paired-end reads were obtained and sequenced on an Illumina Hiseq platform.

125 **Analysis of differentially expressed gene (DEG)**

126 Prior to DEG analysis, the gene expression statistics were analyzed using RSEM software
127 (<http://deweylab.github.io/RSEM/>) to convert the read count numbers to Fragments Per Kilobase
128 of transcript per Million fragments mapped (FPKM), and Principal Component Analysis (PCA)
129 analysis was conducted to determine the similarities and differences in the data. DEGs of the
130 three groups of mice were analyzed as previously described (Shi et al. 2017) using DESeq
131 software (<http://www.bioconductor.org/>). Benjamini and Hochberg's approach was used to
132 control the false discovery rate and adjust the P-values. The adjusted P-value < 0.05 was defined
133 as a standard for significant differences in gene expression. In addition to FPKM hierarchical
134 clustering analysis of DEGs, we further analyzed the subclusters based on \log_2 (ratios) of their
135 gene expression level relative to that of sham group. The \log_2 (ratios) in the SCI_C group ≥ 1 or
136 ≤ -1 was used as a cut-off for subcluster analysis. The clustering algorithm divided the DEGs
137 with similar gene expression trends into several subclusters.

138 **Gene Ontology (GO) and Kyoto Encyclopedia of Genes and Genomes (KEGG) enrichment** 139 **analysis of DEGs**

140 The GO and KEGG analysis were performed using a Goseq R package and KOBAS software as
141 previously described (Shi et al. 2017). In GO analysis, DEGs were implemented using the
142 Goseq R package and gene length bias was corrected. GO terms with corrected P value ≤ 0.05
143 were considered significantly enriched by DEGs. KEGG is a database resource for understanding
144 the high-level functions and utilities of the biological system (<http://www.genome.jp/kegg/>). In
145 this study, we used KOBAS software to test the statistical enrichment of DEGs in KEGG
146 pathways.

147 **Real-time quantitative reverse-transcriptase polymerase chain reaction (RT-qPCR)**

148 To validate RNA-Seq results, 9 DEGs were randomly selected and verified via RT-qPCR
149 according to our previous methods (Shi et al. 2017). The analysis was performed in 6 samples,
150 which included 3 independent samples and duplicates of these samples to be used in RNA-seq
151 analysis. PCR primer sequences are listed in Table 1. The relative quantitative results of each
152 group of genes were calculated according to the formula “ $\Delta\Delta Ct$ ” (Livak & Schmittgen 2001).
153 The statistical values (n=6/group) were presented as mean \pm standard deviation (SD). The data
154 were analyzed using one-way Analysis of Variance (ANOVA), followed by Student–Newman–
155 Keuls tests. Statistical differences were considered significant at $P < 0.05$.

156

157 **Results**

158 **Identification of expressed transcripts the mice spinal cords**

159 For the high quality assessment of sequencing data, nine cDNA libraries were established,
160 including sham (sham_1, sham_2 and sham_3), SCI_C (SCI_C1, SCI_C2 and SCI_C3) and
161 SCI_P (SCI_P1, SCI_P2 and SCI_P3). RNA-Seq produced 48,848,744 - 61,037,096 raw reads
162 for each sample. After filtering out the low-quality reads, there were 48,226,002 - 60,037,772
163 clean reads, with the Q30 (%) 93.67 - 94.31 (Table 2).

164 In order to identify the source of variation within the original data, PCA analysis was conducted.
165 As shown in Fig.1, PC1, PC2 and PC3 were 54.51, 12.33 and 7.09%, respectively. Although not
166 too far from one another, the distance between SCI_C (or SCI_P) and sham was apparent and
167 sufficient for the analysis. These distances demonstrated that the data could be used for the next
168 analysis.

169 **Effect of SCI and probenecid treatment on gene expression**

170

171

172 RPKM and DEGSeq were used to analyze the gene expression level and differential expression
173 profiles, respectively. The results showed that, as compared to the sham group, there were 4,617
174 DEGs in the SCI_C group, including 2,904 upregulated and 1,713 downregulated genes (Fig.2A
175 and Table S1). Compared to the SCI_C group, there were 641 different genes in the SCI_P
176 group, 286 were upregulated and 355 were downregulated (Fig.2B and Table S1). The sequence
177 data have been deposited into Sequence Read Archive
178 (<https://www.ncbi.nlm.nih.gov/sra/PRJNA554464>).

179 **RT-qPCR identification of DEGs**

180 In order to verify the RNA-Seq results, nine DEGs were randomly selected from the SCI_P
181 group, as compared with the SCI_C group, namely Itga1, Lamb1, Cldn5, Lama2, CD34, Esam,
182 Setdb2, Agrn and Ccnt2. The RNA-Seq and RT-qPCR results indicated that the expression
183 patterns of these DEGs were similar (Fig.3).

184 **Cluster Analysis of DEGs**

185 The DEGs from different groups were analyzed using FPKM hierarchical cluster analysis. As
186 shown in Fig. 4, DEGs were hierarchically clustered and classified into different expression
187 clusters. These clusters contained upregulated or downregulated DEGs. When compared to the
188 sham group, most upregulated DEGs in the SCI_C group were in the middle and upper clusters,
189 while downregulated DEGs were delegated to the lower cluster. Additionally, compared to the
190 sham group, most upregulated DEGs in the SCI_P group were in the upper cluster, while
191 downregulated DEGs were mainly observed in the lower cluster. When compared to the SCI_C
192 group, some upregulated DEGs in the SCI_P group were observed in upper cluster, while

193 downregulated DEGs were observed in the middle cluster (there were also some clusters in this
194 grouping that showed no significant differences).

195 In addition to FPKM hierarchical clustering analysis of DEGs, the subclusters — which have
196 similar expression trends — were further analyzed. The \log_2 (ratios) in the SCI_C group ≥ 1 or \leq
197 -1 was used as a cut-off for subcluster analysis. As shown in Fig. 5, we found several subclusters
198 with similar expression trends. Based on \log_2 (ratios) of their gene expression levels relative to
199 that of the sham group, the \log_2 (ratios) of all gene expression levels in the sham group were
200 zero. Fig. 5 A and B show that the two subclusters were strongly upregulated following SCI and
201 then downregulated upon probenecid treatment. Fig. 5 C and D show that the two subclusters
202 were strongly downregulated following SCI and then upregulated upon probenecid treatment. In
203 Fig. 5A, six genes (Cybb, Esam, Itgam, Itgb2, Msn and Ncf2) are demonstrated to have been
204 involved in the leukocyte transendothelial migration signaling pathway; six genes (Col4a1,
205 Erb2, Flt4, Nos3, Syk and Thbs4) were also involved in the PI3K-Akt signaling pathway. Fig.
206 5B displays three genes (Cyba, Ncf1 and Rac2) involved in the NADPH oxidases, two genes
207 (Cflar and Tnfrsf10b) involved in the TRAIL signaling pathway and eight genes (Cd63, Cyba,
208 Ddx58, Fcer1g, Lyn, Myh9, Ncf1 and Psmb8) involved in the innate immune system. Fig. 5C
209 and D show that no gene can be clustered into valuable signaling pathways.

210 **GO enrichment analysis of DEGs**

211 When compared with the sham group, there were seventy-eight GO terms in upregulated DEGs
212 (Fig.6A, Table S2) and nine GO terms in downregulated DEGs (Fig.6B, Table S2) in the SCI_C
213 group. The upregulated DEGs were most enriched in: binding, protein binding, chemokine
214 activity, chemokine receptor binding, G-protein coupled receptor binding, anion binding, small
215 GTPase mediated signal transduction, immune system process, immune response. The

216 downregulated DEGs were most enriched in: protein binding, binding, extracellular-glutamate-
217 gated ion channel activity, acid phosphatase activity, transporter activity, mannose metabolic
218 process, excitatory extracellular ligand-gated ion channel activity, transmembrane transporter
219 activity, anion transmembrane and transporter activity. In the SCI_P group, we observed three
220 GO terms in downregulated DEGs (Fig.6C, Table S3) and no valuable terms in upregulated
221 DEGs (Table S3) compared to the SCI_C group. The downregulated DEGs were protein
222 binding, binding and sequence-specific DNA binding.

223 **KEGG enrichment analysis of DEGs**

224 Scatter plots were used to express the KEGG enrichment analysis results for the DEGs. When
225 compared to the sham group, the upregulated DEGs in the SCI_C group were most enriched in
226 TNF, NF-kappa B, cytokine-cytokine receptor interaction, Toll-like receptor, Leukocyte
227 transendothelial migration, PI3K-Akt, Focal adhesion and apoptosis. (Fig.7A, Table S4); the
228 downregulated DEGs were most enriched in glutamatergic synapse, basal cell carcinoma, axon
229 guidance, other glycan degradation and nicotine addiction (Fig.7B, Table S4). In the SCI_P
230 group vs. SCI_C group, only the “ECM-receptor interaction” was enriched in the upregulated
231 DEGs (Fig.7C, Table S5); the downregulated DEGs were enriched in cell adhesion molecules
232 (CAMs), malaria, leukocyte transendothelial migration, ECM-receptor interaction, PI3K-Akt
233 signaling pathway, hematopoietic cell lineage, focal adhesion, Rap1 signaling pathway and
234 amoebiasis (Fig.7D, Table S5).

235

236 **Discussion**

237 Recent studies have shown that probenecid has neuroprotective and repairing effects on brain
238 disorders (Wei et al. 2015; Xiong et al. 2014). However, its effect on genome-wide transcription

239 in SCI is still unknown. Therefore, in this study, RNA-Seq was used to analyze the effect of
240 probenecid on the local expression of gene transcription eight hours after SCI. The results
241 showed that when compared with the sham group, there were 4,617 DEGs in the SCI_C group,
242 including 2,904 upregulated and 1,713 downregulated genes. When compared with the SCI_C
243 group, there were 641 DEGs in the SCI_P group, 286 of which were upregulated and 355
244 downregulated. These are consistent with others' and our previous reports (Chen et al. 2013; Shi
245 et al. 2017). It also shows that the results of this experiment are reliable. As compared to the
246 SCI_C, there were 641 DEGs in the SCI_P group, 286 were upregulated and 355 were
247 downregulated. To further verify the RNA-seq results, we randomly selected 9 DEGs (Itga1,
248 Lamb1, Cldn5, Lama2, CD34, Esam, Setdb2, Agrn and Ccnt2) for RT-qPCR. The results
249 showed that the expression patterns of these genes detected by these two methods were similar,
250 indicating that our RNA-seq results are reliable and can be used for subsequent analysis. These
251 also confirmed that probenecid can alter gene transcription after SCI.

252 To further analyze the DEGs effected by probenecid, we used GO enrichment to reflect the
253 distribution of DEGs on GO term enriched in cell components, molecular functions and
254 biological processes (Huang et al. 2013). In the SCI_P vs. SCI_C group, analysis showed that
255 there were 3 GO terms in downregulated DEGs (protein binding, binding and sequence-specific
256 DNA binding) and no valuable terms in upregulated DEGs. KEGG analysis showed that the
257 valuable signaling pathways associated with these DEGs included: CAMs, leukocyte
258 transendothelial migration, ECM-receptor interaction, PI3K-Akt signaling pathway,
259 hematopoietic cell lineage, focal adhesion, and Rap1 signaling pathway, ete.

260 Among these signal pathways, some are known to be related to SCI, such as CAMs (Brook et al.
261 2000; Zhang et al. 2008), ECM-receptor interaction (Zhou et al. 2017), PI3K-Akt signaling

262 pathway (Li et al. 2019a; Li et al. 2019b; Zhang et al. 2017) and focal adhesion (Chuang et al.
263 2018; Graham et al. 2016; Hao et al. 2018).

264 Following SCI, probenecid treatment could downregulate some genes, subclusters and signaling
265 pathways. Leukocyte transendothelial migration from the blood into tissues is vital for immune
266 surveillance and inflammation (Cook-Mills 2006). However there is a large amount of leukocyte
267 infiltration involved in the pathological process of SCI. These infiltrating leukocytes need to bind
268 to endothelial cell adhesion molecules and then migrate between vascular endothelial cells
269 (Wang et al. 2011). Therefore, the inhibition of leukocyte transendothelial migration and CAMs
270 induced by probenecid may play a role in inhibiting inflammation by weakening the infiltration
271 of white blood cells in the injured area. In this study, we clustered six genes (Cybb, Esam, Itgam,
272 Itgb2, Msn and Ncf2) involved in this pathway. Their expression is strongly downregulated
273 following SCI and then upregulated upon probenecid treatment. This demonstrates that
274 probenecid treatment following SCI can play an anti-inflammatory role by inhibiting the
275 infiltration of inflammatory cells.

276 The ECM plays an important role in tissue and organ morphogenesis (Bonnans et al. 2014;
277 Rabelink et al. 2017) and control of cellular activities such as adhesion, migration,
278 differentiation, proliferation and apoptosis (Yue 2014). Focal adhesions are specialized,
279 intracellular sites in which aggregated integrin receptors interact with extracellular matrices,
280 while extracellular matrices interact with intracellular actin cytoskeleton (Burrige 2017;
281 LaFlamme et al. 2018). At the same time, focal adhesions are the result of cell and extracellular
282 matrix (ECM) interactions (Burrige 2017; De Pascalis & Etienne-Manneville 2017). ECM and
283 focal adhesions are downregulated after probenecid treatment, indicating that probenecid might
284 improve SCI by inhibiting adhesion, migration, differentiation, proliferation and apoptosis.

285 It has been reported that PI3K-Akt signaling fuses a variety of extracellular and intracellular
286 signal transduction pathways that regulate macrophage biology, including: the production of pro-
287 inflammatory cytokines, phagocytosis, autophagy and homeostasis (Vergadi et al. 2017). PI3K-
288 Akt signal pathway is downregulated in SCI after probenecid treatment, and the six genes
289 (Col4a1, Erbb2, Flt4, Nos3, Syk and Thbs4) being clustered into this pathway indicate that
290 probenecid might improve SCI by regulating macrophages and inhibiting inflammatory
291 pathways. This is likely to provide important clues towards identifying the mechanism by which
292 probenecid acts.

293 The relationship between the hematopoietic cell lineage pathway and SCI was referred to in a
294 report on the bioinformatics analysis of SCI (Zhu et al. 2017). Its specific role has yet to be
295 reported and requires further discussion.

296 Rap1 signal pathway plays an important role in regulating cell-cell and cell-matrix interactions
297 by regulating the function of adhesion molecules (Kim et al. 2011; Pollan et al. 2018). In our
298 study, Rap1 signaling pathways were enriched in downregulated DEGs of SCI after probenecid
299 treatment, suggesting that probenecid may inhibit cell adhesion and polarization by inhibiting the
300 Rap1 signaling pathway, thereby inhibiting inflammation.

301 In addition, three genes (Cyba, Ncf1 and Rac2) related to the NADPH oxidases, two genes (Cflar
302 and Tnfrsf10b) related to the TRAIL signaling pathway and eight genes (Cd63, Cyba, Ddx58,
303 Fcer1g, Lyn, Myh9, Ncf1 and Psmb8) related to the innate immune system were also strongly
304 downregulated following probenecid treatment. We know that NADPH oxidases are involved in
305 oxidative stress, the TRAIL signaling pathway mediates inflammation and apoptosis and the
306 immune system is involved in almost all pathological processes of injury (Chyuan et al. 2018;
307 Ewald 2018; Tisato et al. 2018). Therefore, probenecid treatment can potentially play a

308 neuroprotective role by inhibiting immune response, oxidative stress, anti-inflammation and anti-
309 apoptosis after SCI.

310 **Conclusions**

311 Acute SCI can lead to changes in the mRNAs of injured spinal cords. These mRNAs and their
312 related pathways can provide some explanation for the pathological mechanism of acute SCI.
313 More interestingly, we also demonstrated that probenecid can lead to gene expression inhibitions
314 in an acute injured spinal cord. These downregulated DEGs and their associated signaling
315 pathways — such as focal adhesions, leukocyte transendothelial migration, ECM-receptor
316 interaction, PI3K-Akt, Rap1 — are mainly related to inflammatory response, local hypoxia,
317 macrophage differentiation, adhesion migration and apoptosis of local cells. This suggests that
318 the application of probenecid in the acute phase can improve the local microenvironment of SCI.
319 However, the application of probenecid as a therapeutic drug for SCI requires further
320 investigation. Next, the detailed research on this subject will be conducted by combining animal
321 models and clinical practice.

322

323 **References**

- 324 Ahuja CS, Nori S, Tetreault L, Wilson J, Kwon B, Harrop J, Choi D, and Fehlings MG. 2017.
325 Traumatic Spinal Cord Injury-Repair and Regeneration. *Neurosurgery* 80:S9-S22.
326 10.1093/neuros/nyw080
- 327 Baranova A, Ivanov D, Petrash N, Pestova A, Skoblov M, Kelmanson I, Shagin D, Nazarenko S,
328 Geraymovych E, Litvin O, Tiunova A, Born TL, Usman N, Staroverov D, Lukyanov S,
329 and Panchin Y. 2004. The mammalian pannexin family is homologous to the invertebrate
330 innexin gap junction proteins. *Genomics* 83:706-716. 10.1016/j.ygeno.2003.09.025
- 331 Bonnans C, Chou J, and Werb Z. 2014. Remodelling the extracellular matrix in development and
332 disease. *Nat Rev Mol Cell Biol* 15:786-801. 10.1038/nrm3904
- 333 Bravo D, Ibarra P, Retamal J, Pelissier T, Laurido C, Hernandez A, and Constandil L. 2014.
334 Pannexin 1: a novel participant in neuropathic pain signaling in the rat spinal cord. *Pain*
335 155:2108-2115. 10.1016/j.pain.2014.07.024
- 336 Brook GA, Houweling DA, Gieling RG, Hermanns T, Joosten EA, Bar DP, Gispen WH, Schmitt
337 AB, Leprince P, Noth J, and Nacimiento W. 2000. Attempted endogenous tissue repair
338 following experimental spinal cord injury in the rat: involvement of cell adhesion
339 molecules L1 and NCAM? *Eur J Neurosci* 12:3224-3238.
- 340 BurrIDGE K. 2017. Focal adhesions: a personal perspective on a half century of progress. *FEBS J*
341 284:3355-3361. 10.1111/febs.14195
- 342 Chen K, Deng S, Lu H, Zheng Y, Yang G, Kim D, Cao Q, and Wu JQ. 2013. RNA-seq
343 characterization of spinal cord injury transcriptome in acute/subacute phases: a resource
344 for understanding the pathology at the systems level. *PLoS One* 8:e72567.
345 10.1371/journal.pone.0072567
- 346 Chuang YC, Lee CH, Sun WH, and Chen CC. 2018. Involvement of advillin in somatosensory
347 neuron subtype-specific axon regeneration and neuropathic pain. *Proc Natl Acad Sci U S*
348 *A* 115:E8557-E8566. 10.1073/pnas.1716470115
- 349 Chyuan IT, Tsai HF, Wu CS, Sung CC, and Hsu PN. 2018. TRAIL-Mediated Suppression of T
350 Cell Receptor Signaling Inhibits T Cell Activation and Inflammation in Experimental
351 Autoimmune Encephalomyelitis. *Front Immunol* 9:15. 10.3389/fimmu.2018.00015
- 352 Cook-Mills JM. 2006. Hydrogen peroxide activation of endothelial cell-associated MMPs during
353 VCAM-1-dependent leukocyte migration. *Cell Mol Biol (Noisy-le-grand)* 52:8-16.
- 354 De Pascalis C, and Etienne-Manneville S. 2017. Single and collective cell migration: the
355 mechanics of adhesions. *Mol Biol Cell* 28:1833-1846. 10.1091/mbc.E17-03-0134
- 356 Du L, Empey PE, Ji J, Chao H, Kochanek PM, Bayir H, and Clark RS. 2016. Probenecid and N-
357 Acetylcysteine Prevent Loss of Intracellular Glutathione and Inhibit Neuronal Death after
358 Mechanical Stretch Injury In Vitro. *J Neurotrauma* 33:1913-1917. 10.1089/neu.2015.4342
- 359 Ewald CY. 2018. Redox Signaling of NADPH Oxidases Regulates Oxidative Stress Responses,
360 Immunity and Aging. *Antioxidants (Basel)* 7. 10.3390/antiox7100130
- 361 Friedli L, Rosenzweig ES, Barraud Q, Schubert M, Dominici N, Awai L, Nielson JL, Musienko
362 P, Nout-Lomas Y, Zhong H, Zdunowski S, Roy RR, Strand SC, van den Brand R, Havton
363 LA, Beattie MS, Bresnahan JC, Bezdard E, Bloch J, Edgerton VR, Ferguson AR, Curt A,
364 Tuszynski MH, and Courtine G. 2015. Pronounced species divergence in corticospinal tract
365 reorganization and functional recovery after lateralized spinal cord injury favors primates.
366 *Sci Transl Med* 7:302ra134. 10.1126/scitranslmed.aac5811
- 367 Geisler FH, Coleman WP, Benzel E, Ducker T, and Hurlbert RJ. 2002. Spinal cord injury. *Lancet*
368 360:1883; author reply 1884. 10.1016/s0140-6736(02)11744-2

- 369 Graham ZA, Qin W, Harlow LC, Ross NH, Bauman WA, Gallagher PM, and Cardozo CP. 2016.
370 Focal adhesion kinase signaling is decreased 56 days following spinal cord injury in rat
371 gastrocnemius. *Spinal Cord* 54:502-509. 10.1038/sc.2015.183
- 372 Hagos FT, Daood MJ, Ocque JA, Nolin TD, Bayir H, Poloyac SM, Kochanek PM, Clark RS, and
373 Empey PE. 2017. Probenecid, an organic anion transporter 1 and 3 inhibitor, increases
374 plasma and brain exposure of N-acetylcysteine. *Xenobiotica* 47:346-353.
375 10.1080/00498254.2016.1187777
- 376 Hainz N, Wolf S, Beck A, Wagenpfeil S, Tschernig T, and Meier C. 2017. Probenecid arrests the
377 progression of pronounced clinical symptoms in a mouse model of multiple sclerosis. *Sci*
378 *Rep* 7:17214. 10.1038/s41598-017-17517-5
- 379 Hao M, Ji XR, Chen H, Zhang W, Zhang LC, Zhang LH, Tang PF, and Lu N. 2018. Cell cycle and
380 complement inhibitors may be specific for treatment of spinal cord injury in aged and
381 young mice: Transcriptomic analyses. *Neural Regen Res* 13:518-527. 10.4103/1673-
382 5374.226405
- 383 Huang Q, Wu LY, Wang Y, and Zhang XS. 2013. GOMA: functional enrichment analysis tool
384 based on GO modules. *Chin J Cancer* 32:195-204. 10.5732/cjc.012.10151
- 385 Kim C, Ye F, and Ginsberg MH. 2011. Regulation of integrin activation. *Annu Rev Cell Dev Biol*
386 27:321-345. 10.1146/annurev-cellbio-100109-104104
- 387 Krueger H, Noonan VK, Trenaman LM, Joshi P, and Rivers CS. 2013. The economic burden of
388 traumatic spinal cord injury in Canada. *Chronic Dis Inj Can* 33:113-122.
- 389 LaFlamme SE, Mathew-Steiner S, Singh N, Colello-Borges D, and Nieves B. 2018. Integrin and
390 microtubule crosstalk in the regulation of cellular processes. *Cell Mol Life Sci* 75:4177-
391 4185. 10.1007/s00018-018-2913-x
- 392 Li H, Zhang X, Qi X, Zhu X, and Cheng L. 2019a. Icariin Inhibits Endoplasmic Reticulum Stress-
393 induced Neuronal Apoptosis after Spinal Cord Injury through Modulating the PI3K/AKT
394 Signaling Pathway. *Int J Biol Sci* 15:277-286. 10.7150/ijbs.30348
- 395 Li Y, Guo Y, Fan Y, Tian H, Li K, and Mei X. 2019b. Melatonin Enhances Autophagy and
396 Reduces Apoptosis to Promote Locomotor Recovery in Spinal Cord Injury via the
397 PI3K/AKT/mTOR Signaling Pathway. *Neurochem Res* 44:2007-2019. 10.1007/s11064-
398 019-02838-w
- 399 Livak KJ, and Schmittgen TD. 2001. Analysis of relative gene expression data using real-time
400 quantitative PCR and the 2(-Delta Delta C(T)) Method. *Methods* 25:402-408.
401 10.1006/meth.2001.1262
- 402 Mawhinney LJ, de Rivero Vaccari JP, Dale GA, Keane RW, and Bramlett HM. 2011. Heightened
403 inflammasome activation is linked to age-related cognitive impairment in Fischer 344 rats.
404 *BMC Neurosci* 12:123. 10.1186/1471-2202-12-123
- 405 McDonald JW, and Sadowsky C. 2002. Spinal-cord injury. *Lancet* 359:417-425. 10.1016/S0140-
406 6736(02)07603-1
- 407 Oyinbo CA. 2011. Secondary injury mechanisms in traumatic spinal cord injury: a nugget of this
408 multiply cascade. *Acta Neurobiol Exp (Wars)* 71:281-299.
- 409 Papadopoulos MC, and Verkman AS. 2008. Potential utility of aquaporin modulators for therapy
410 of brain disorders. *Prog Brain Res* 170:589-601. 10.1016/S0079-6123(08)00446-9
- 411 Pineda-Farias JB, Perez-Severiano F, Gonzalez-Esquivel DF, Barragan-Iglesias P, Bravo-
412 Hernandez M, Cervantes-Duran C, Aguilera P, Rios C, and Granados-Soto V. 2013. The
413 L-kynurenine-probenecid combination reduces neuropathic pain in rats. *Eur J Pain*
414 17:1365-1373. 10.1002/j.1532-2149.2013.00305.x

- 415 Pollan SG, Huang F, Sperger JM, Lang JM, Morrissey C, Cress AE, Chu CY, Bhowmick NA, You
416 S, Freeman MR, Spassov DS, Moasser MM, Carter WG, Satapathy SR, Shah K, and
417 Knudsen BS. 2018. Regulation of inside-out beta1-integrin activation by CDCP1.
418 *Oncogene* 37:2817-2836. 10.1038/s41388-018-0142-2
- 419 Qiu J. 2009. China Spinal Cord Injury Network: changes from within. *Lancet Neurol* 8:606-607.
420 10.1016/S1474-4422(09)70162-0
- 421 Rabelink TJ, van den Berg BM, Garsen M, Wang G, Elkin M, and van der Vlag J. 2017.
422 Heparanase: roles in cell survival, extracellular matrix remodelling and the development
423 of kidney disease. *Nat Rev Nephrol* 13:201-212. 10.1038/nrneph.2017.6
- 424 Shi LL, Zhang N, Xie XM, Chen YJ, Wang R, Shen L, Zhou JS, Hu JG, and Lu HZ. 2017.
425 Transcriptome profile of rat genes in injured spinal cord at different stages by RNA-
426 sequencing. *BMC Genomics* 18:173. 10.1186/s12864-017-3532-x
- 427 Singh A, Tetreault L, Kalsi-Ryan S, Nouri A, and Fehlings MG. 2014. Global prevalence and
428 incidence of traumatic spinal cord injury. *Clin Epidemiol* 6:309-331.
429 10.2147/CLEP.S68889
- 430 Tisato V, Gallo S, Melloni E, Celeghini C, Passaro A, Zauli G, Secchiero P, Bergamini C, Trentini
431 A, Bonaccorsi G, Valacchi G, Zuliani G, and Cervellati C. 2018. TRAIL and
432 Ceruloplasmin Inverse Correlation as a Representative Crosstalk between Inflammation
433 and Oxidative Stress. *Mediators Inflamm* 2018:9629537. 10.1155/2018/9629537
- 434 Tollner K, Brandt C, Romermann K, and Loscher W. 2015. The organic anion transport inhibitor
435 probenecid increases brain concentrations of the NKCC1 inhibitor bumetanide. *Eur J*
436 *Pharmacol* 746:167-173. 10.1016/j.ejphar.2014.11.019
- 437 Tran AP, Warren PM, and Silver J. 2018. The Biology of Regeneration Failure and Success After
438 Spinal Cord Injury. *Physiol Rev* 98:881-917. 10.1152/physrev.00017.2017
- 439 Vergadi E, Ieronymaki E, Lyroni K, Vaporidi K, and Tsatsanis C. 2017. Akt Signaling Pathway
440 in Macrophage Activation and M1/M2 Polarization. *J Immunol* 198:1006-1014.
441 10.4049/jimmunol.1601515
- 442 Wang JG, Williams JC, Davis BK, Jacobson K, Doerschuk CM, Ting JP, and Mackman N. 2011.
443 Monocytic microparticles activate endothelial cells in an IL-1beta-dependent manner.
444 *Blood* 118:2366-2374. 10.1182/blood-2011-01-330878
- 445 Wei R, Wang J, Xu Y, Yin B, He F, Du Y, Peng G, and Luo B. 2015. Probenecid protects against
446 cerebral ischemia/reperfusion injury by inhibiting lysosomal and inflammatory damage in
447 rats. *Neuroscience* 301:168-177. 10.1016/j.neuroscience.2015.05.070
- 448 Xiong XX, Gu LJ, Shen J, Kang XH, Zheng YY, Yue SB, and Zhu SM. 2014. Probenecid protects
449 against transient focal cerebral ischemic injury by inhibiting HMGB1 release and
450 attenuating AQP4 expression in mice. *Neurochem Res* 39:216-224. 10.1007/s11064-013-
451 1212-z
- 452 Yue B. 2014. Biology of the extracellular matrix: an overview. *J Glaucoma* 23:S20-23.
453 10.1097/IJG.000000000000108
- 454 Zhang F, Ru N, Shang ZH, Chen JF, Yan C, Li Y, and Liang J. 2017. Daidzein ameliorates spinal
455 cord ischemia/reperfusion injury-induced neurological function deficits in Sprague-
456 Dawley rats through PI3K/Akt signaling pathway. *Exp Ther Med* 14:4878-4886.
457 10.3892/etm.2017.5166
- 458 Zhang Y, Yeh J, Richardson PM, and Bo X. 2008. Cell adhesion molecules of the immunoglobulin
459 superfamily in axonal regeneration and neural repair. *Restor Neurol Neurosci* 26:81-96.

460 Zhou J, Xiong Q, Chen H, Yang C, and Fan Y. 2017. Identification of the Spinal Expression Profile
461 of Non-coding RNAs Involved in Neuropathic Pain Following Spared Nerve Injury by
462 Sequence Analysis. *Front Mol Neurosci* 10:91. 10.3389/fnmol.2017.00091Zhu Z, Wang
463 D, Jiao W, Chen G, Cao Y, Zhang Q, and Wang J. 2017. Bioinformatics analyses of
464 pathways and gene predictions in IL-1alpha and IL-1beta knockout mice with spinal cord
465 injury. *Acta Histochem* 119:663-670. 10.1016/j.acthis.2017.07.007
466

467 **Figures**

468 **Figure 1 PCA analysis**

469
470
471 PCA analysis was performed using three principal components (PC1, 2 and 3) to demonstrate the
472 source of variance (n=3).
473

474 **Figure 2 Volcano map of DEGs**

475
476 Red, green and blue dots represent significantly upregulated, downregulated and unchanged gene
477 expressions, respectively. (A) SCI_C vs Sham; (B) SCI_P vs SCI_C.
478

479 **Figure 3 RT-qPCR verification of DEGs characterized by RNA-Seq**

480
481 A: The longitudinal coordinates in RNA-Seq are mRNA expression levels (read counts, n = 3). B:
482 The longitudinal coordinates in RT-qPCR are mRNA expression level calculated using the “ $\Delta\Delta Ct$ ”
483 method and expressed relative to the value in the sham group (designated as 1). All data were
484 calculated with mean \pm standard deviation (n = 6, which included 3 independent samples and the
485 3 same samples used for the RNA-seq analysis). **P < 0.01 (ANOVA).
486

487 **Figure 4 Hierarchical cluster analysis of DEGs**

488
489 The DEGs in different groups were analyzed using FPKM hierarchical cluster analysis. The read
490 count numbers of FPKM were converted using a RSEM software. DEGs were classified into
491 different expression cluster by hierarchical clustering. The colour scheme (red to blue) represents
492 the up-to-down of the gene expression. sham: sham group; SCI_C: SCI (solvent control) group;
493 SCI_P: SCI (probenecid) group.
494

495 **Figure 5 Subcluster analysis of DEGs**

496 The subclusters of DEGs which have similar expression trends were further analyzed. The log₂
497 (ratios) in SCI_C group ≥ 1 or ≤ -1 was used as a cut-off. Based on log₂ (ratios) of the gene
498 expression level relative to that of sham group, the log₂ (ratios) of all gene expression levels in
499 sham group were zero. A and B: the two subclusters which were strongly upregulated following
500 SCI and then downregulated upon probenecid treatment. C and D: the two subclusters which
501 were strongly downregulated following SCI and then upregulated upon probenecid treatment.
502

503 **Figure 6 GO enrichment analysis of DEGs**

504

505 DEGs were implemented by the Goseq R package, in which gene length bias was corrected. GO
506 terms with corrected P value ≤ 0.05 were considered significantly enriched by DEGs. The asterisk
507 (*) represents significant enrichment terms ($P \leq 0.05$). A: GO analysis of upregulated DEGs in
508 SCI_C vs sham group; B: GO analysis of downregulated DEGs in SCI_C vs sham group; C: GO
509 analysis of downregulated DEGs in SCI_P vs SCI_C group.

510

511 **Figure 7 KEGG enrichment analyses of DEGs**

512

513 KOBAS software was used to test the statistical enrichment of DEGs in KEGG pathways. In this
514 figure, KEGG enrichment is measured by Rich factor, Qvalue and the number of genes enriched
515 in the related pathway. Rich factor refers to the ratio of the number of differentiated genes
516 (sample number) enriched in the pathway to the number of annotated genes (background
517 number). The larger the Rich factor, the greater the degree of enrichment. Qvalue is the Pvalue
518 after multiple hypothesis test correction. The range of Qvalue is between 0 and 1. The closer the
519 Qvalue is to 0, the more significant the enrichment is. The KEGG pathways were shown in A:
520 upregulated DEGs (SCI_C vs sham); B: downregulated DEGs; C: upregulated DEGs (SCI_P vs
521 SCP_C); D: downregulated DEGs (SCI_C vs sham).

522

523 **Tables**

524

525 Table 1 PCR primers used in the study

526 Table 2 Summary of sequence assembly after Illumina sequencing

527

528 **Supplementary materials**

529 Table S1 DEGs of different groups

530 Table S2 GO enrichment analysis of SCI_C vs sham group

531 Table S3 GO enrichment analysis of SCI_P vs SCI_C group

532 Table S4 KEGG analysis of SCI_C vs sham group

533 Table S5 KEGG analysis of SCI_P vs SCI_C group

534

535

Figure 1

Figure 1 PCA analysis

PCA analysis was performed using three principal components (PC1, 2, and 3) to demonstrate the source of variance (n=3).

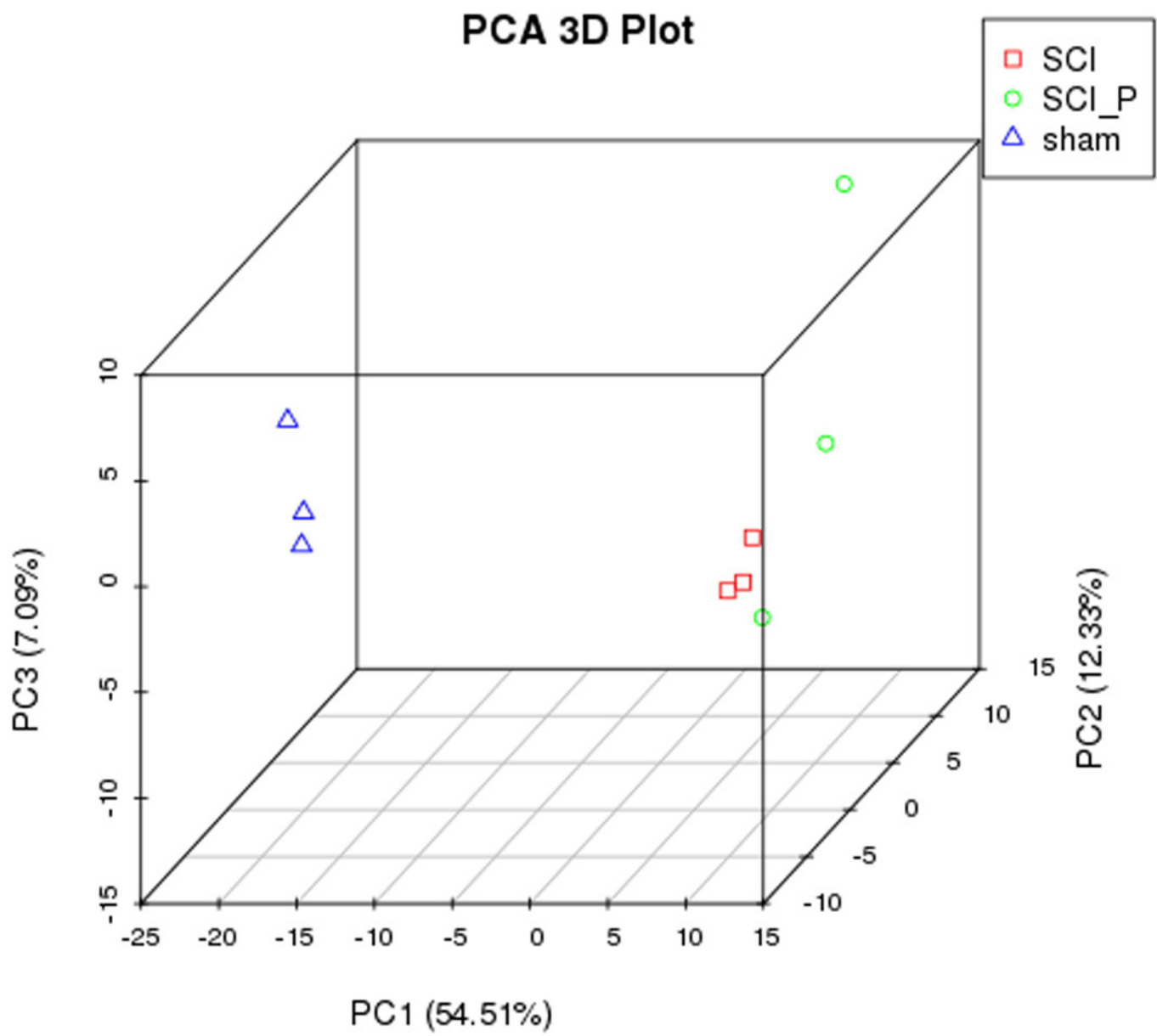


Figure 2

Figure 2 Volcano map of DEGs

Red, green and blue dots represent significantly upregulated, downregulated and no changed gene expressions, respectively. (A) SCI_C vs Sham; (B) SCI_P vs SCI_C.

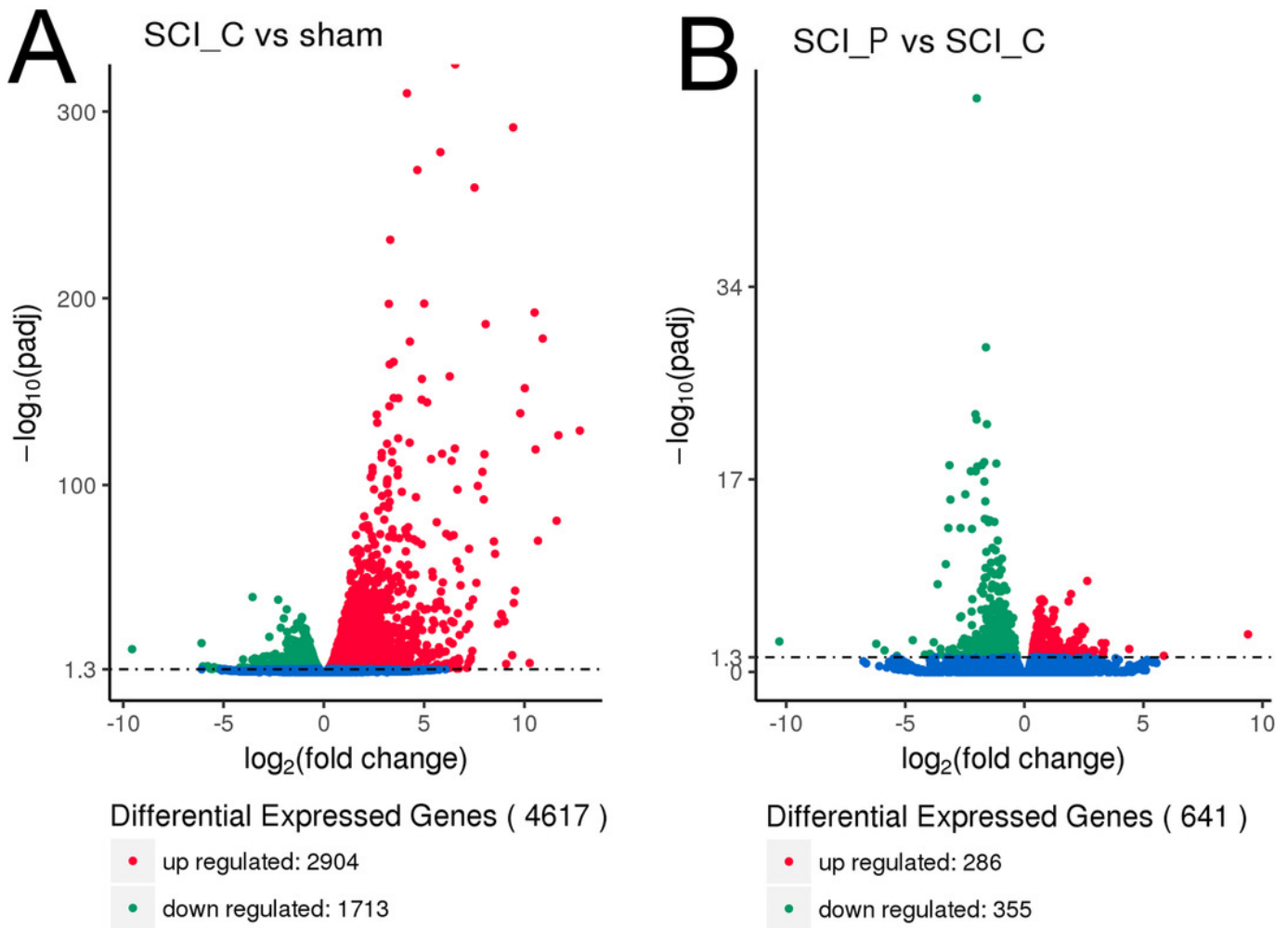


Figure 3

Figure 3 RT-qPCR verification of DEGs characterized by RNA-Seq

A: The longitudinal coordinates in RNA-Seq were the mRNA expression level (read counts, $n = 3$). B: The longitudinal coordinates in RT-qPCR were the mRNA expression level calculated using the $\Delta\Delta\text{Ct}$ method and expressed relative to the value in the sham group (designated as 1). All data were calculated with mean \pm standard deviation ($n = 6$, which included 3 independent samples and the 3 same samples used for the RNA-seq analysis). $**P < 0.01$ (ANOVA).

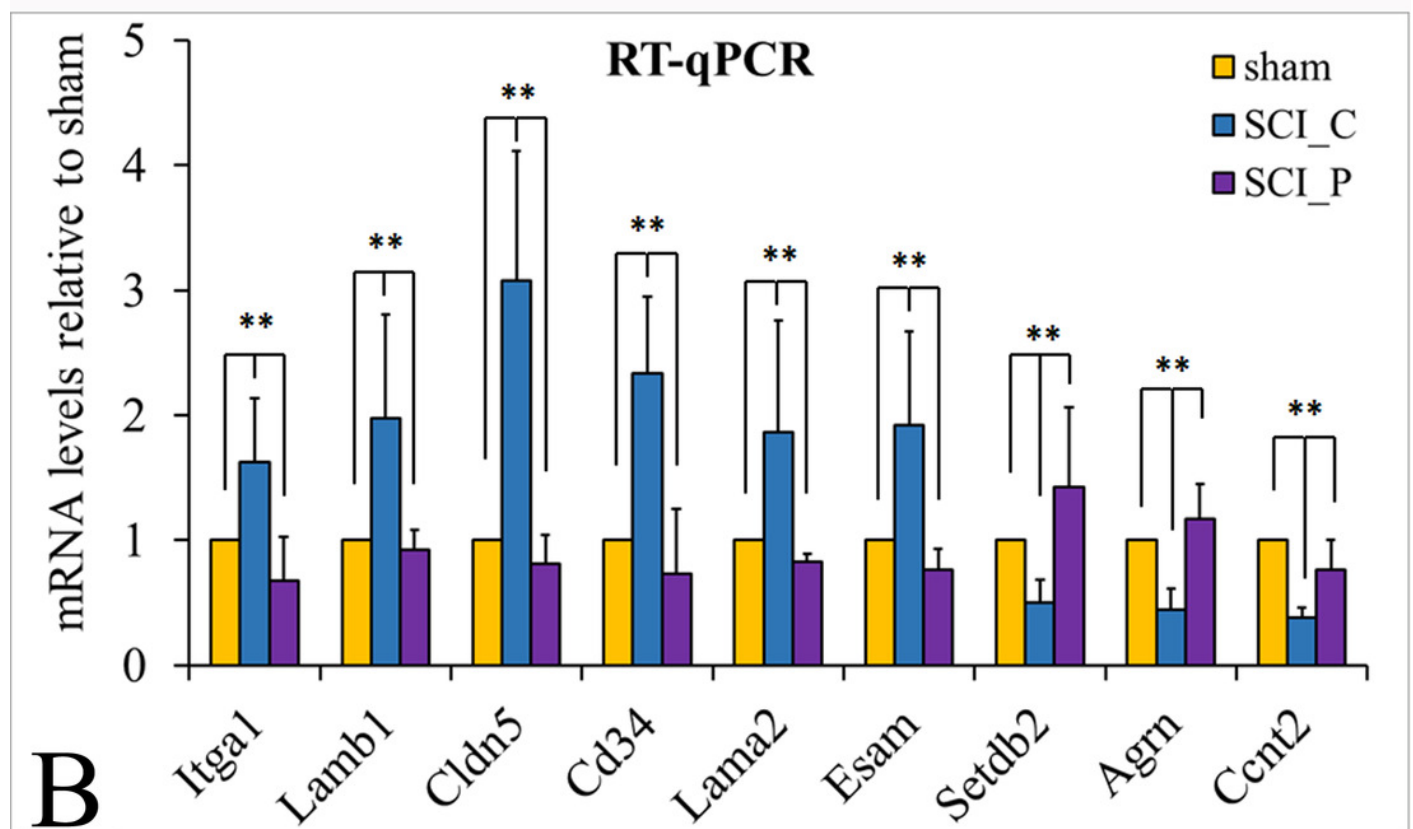
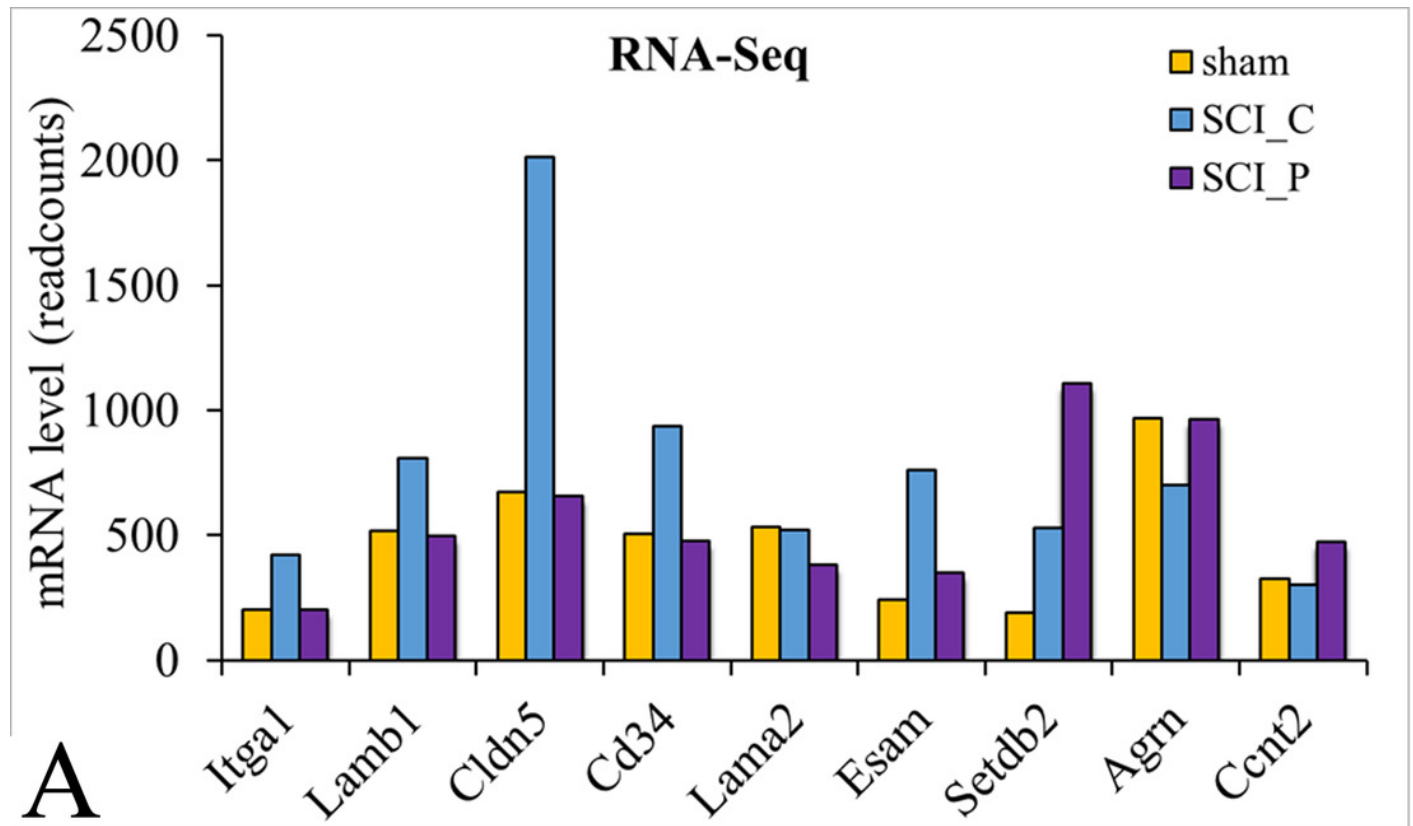


Figure 4

Figure 4 Hierarchical cluster analysis of DEGs

The DEGs in different groups were analyzed using FPKM hierarchical cluster analysis. The read count numbers of FPKM were converted by RSEM software. DEGs were classified into different expression cluster by hierarchical clustering. The colour scheme (red to blue) represents the up to down of the gene expression. sham: sham group; SCI_C: SCI (solvent control) group; SCI_P: SCI (probenecid) group.

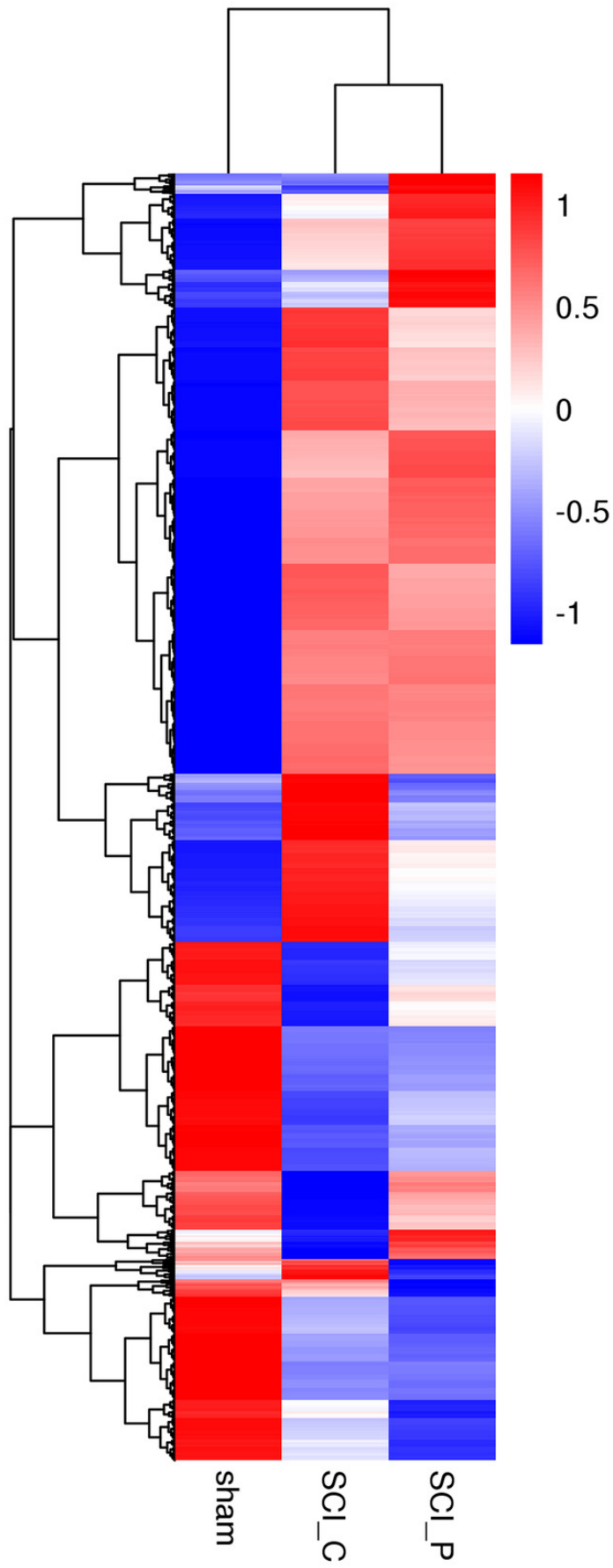


Figure 5

Figure 5 Subcluster analysis of DEGs

The subclusters of DEGs which have similar expression trends were further analyzed. The \log_2 (ratios) in SCI_C group ≥ 1 or ≤ -1 was used as a cut-off. Based on \log_2 (ratios) of the gene expression level relative to that of sham group, the \log_2 (ratios) of all gene expression levels in sham group were zero. A and B: the two subclusters which were strongly upregulated following SCI, and then downregulated upon probenecid treatment. C and D: the two subclusters which were strongly downregulated following SCI, and then upregulated upon probenecid treatment.

A

Name	sham	SCI	CSCI	P
Rgs16	0	1.78	1.07	
Col4a1	0	1.7	0.9	
Apobec3	0	1.66	1.29	
Syk	0	1.65	0.89	
Akr1b8	0	1.64	1.18	
Ifi35	0	1.62	1.21	
Thbs4	0	1.61	1.2	
Esam	0	1.61	0.49	
Pstpip2	0	1.59	0.58	
Sdc1	0	1.58	1.05	
Gda	0	1.58	0.85	
A2m	0	1.57	1.42	
Dok2	0	1.57	0.66	
Nupr1	0	1.57	0.85	
Aoc3	0	1.57	-0.41	
Zfp429	0	1.54	0.65	
Lox4	0	1.53	1.05	
Capg	0	1.52	0.9	
Tnfrsf11b	0	1.52	1.37	
Timeless	0	1.51	1.09	
Plek	0	1.51	0.96	
Naip2	0	1.51	1.22	
Arhgef5	0	1.49	0.59	
Slc1a5	0	1.48	0.68	
Plekha2	0	1.48	0.83	
Anxa2	0	1.47	1.05	
Cyp11b1	0	1.47	0.85	
Tbx3	0	1.46	0.29	
Tmem154	0	1.45	1	
Emp3	0	1.44	1.12	
Ptprc	0	1.43	0.57	
Ets1	0	1.42	0.68	
Mgp	0	1.41	0.28	
Il33	0	1.41	0.85	
Acat3	0	1.41	0.98	
Anxa3	0	1.4	0.97	
Cd52	0	1.4	0.22	
Ltrb	0	1.4	1.06	
Gjc1	0	1.4	0.87	
Igfbp7	0	1.39	0.47	
Stom	0	1.39	0.91	
Gpr182	0	1.39	0.46	
Hmg2	0	1.39	0.81	
Steap3	0	1.39	0.73	
Nef2	0	1.37	0.96	
Plp2	0	1.37	0.77	
Phf11d	0	1.37	1.09	
Nos3	0	1.35	0.06	
Hspa4l	0	1.35	0.79	
Adam12	0	1.34	0.82	
Tgfb1	0	1.34	0.57	
Rdh12	0	1.33	0.66	
Marveld2	0	1.33	0.91	
Alox5ap	0	1.3	0.03	
Ap1s3	0	1.29	1.03	
Ampd1	0	1.29	-1.8	
Irgb2	0	1.29	0.33	
Ip6k3	0	1.28	1.04	
Snx20	0	1.28	0.5	
Flt4	0	1.27	0.31	
Spil	0	1.26	0.71	
Fblim1	0	1.24	0.81	
Filip1l	0	1.24	0.41	
Was	0	1.22	0.99	
Arhgap30	0	1.22	0.83	
Slc39a1	0	1.21	0.96	
Rin3	0	1.21	0.39	
Emilin1	0	1.21	0.7	
Erg	0	1.21	0.13	
Entpd1	0	1.2	0.46	
Notch4	0	1.2	0.43	
Pear1	0	1.19	0.08	
Hcls1	0	1.18	0.76	
Nfam1	0	1.17	0.49	
Parp10	0	1.16	0.81	
Dkk2	0	1.15	-0.12	
Zfp217	0	1.15	0.79	
Iqgap1	0	1.14	0.64	
Ierf1	0	1.14	0.71	
Msn	0	1.13	0.73	
Icam2	0	1.13	0.1	
Ilgam	0	1.13	0.57	
Plekha4	0	1.12	-0.33	
Irf8	0	1.12	0.25	
C1ra	0	1.12	0.47	
Atp10a	0	1.11	0.51	
Slc25a24	0	1.1	0.74	
Cd33	0	1.1	0.68	
Tarm1	0	1.1	0.24	
Kcnj8	0	1.1	0.38	
Hmgcs2	0	1.09	-0.61	
Trim56	0	1.07	0.73	
Sp100	0	1.07	-0.1	
Tpm6	0	1.07	0.39	
Erb2	0	1.06	0.45	
Id3	0	1.06	0.51	
Tbxa2r	0	1.05	-0.96	
Foxq1	0	1.05	-0.44	
Myo1c	0	1.05	0.6	
Arhgdib	0	1.05	0.34	
Fbln2	0	1.04	0.3	
Apobp	0	1.04	0.37	
Hk3	0	1.04	0.5	
Fxyd3	0	1.02	-0.32	
Cybb	0	1	-0.71	
Prrh1	0	1	0.33	

B

Name	sham	SCI	CSCI	P
Sox7	0	1.49	0.65	
S100a6	0	1.48	1.34	
Tnfrsf10b	0	1.48	0.96	
Lyn	0	1.42	1.2	
Trib3	0	1.4	1.03	
Tpm4	0	1.39	1.02	
Rac2	0	1.36	1.06	
Tec	0	1.3	1.15	
Wwtr1	0	1.29	1.03	
Slc5a3	0	1.27	1.09	
Yap1	0	1.27	0.98	
Feer1g	0	1.26	1.06	
Ecm1	0	1.25	0.61	
Ptpn12	0	1.25	1.08	
Itpr1p1	0	1.23	0.86	
Gpd1	0	1.22	1.1	
Id1	0	1.2	0.62	
S100a10	0	1.19	1	
Met	0	1.18	1.01	
Wisp1	0	1.18	1.01	
Slc2a1	0	1.18	0.72	
Twist1	0	1.17	0.26	
Mb21d1	0	1.17	0.88	
Ddx58	0	1.16	1.02	
Layn	0	1.16	1.12	
Tmem37	0	1.16	0.51	
Cavin1	0	1.15	0.65	
Ldha	0	1.14	0.74	
Lrrn4cl	0	1.14	0.28	
Cyba	0	1.14	0.56	
Adipor2	0	1.13	0.97	
Myh9	0	1.12	0.79	
Casp12	0	1.12	0.99	
Vsig2	0	1.11	0.4	
Fhl3	0	1.11	0.9	
Rhoc	0	1.11	0.91	
Rbpms	0	1.1	0.29	
Lrrc8a	0	1.1	0.98	
Xbp1	0	1.1	0.64	
Susd6	0	1.09	0.98	
Cdc42se1	0	1.07	1	
Myo1g	0	1.07	0.69	
Rph3al	0	1.07	0.72	
Nfya	0	1.06	-0.11	
Cflar	0	1.05	0.67	
Psmb8	0	1.04	0.7	
Vgf	0	1.04	0.69	
Dll4	0	1.03	0.42	
Tnfaip8l1	0	1.03	0.84	
Ncf1	0	1.03	0.77	
Gypc	0	1.02	0.74	
Cd63	0	1.02	0.86	
Psd4	0	1.01	0.72	
Tspo	0	1	0.56	

C

Name	sham	SCI	CSCI	P
Snmp40	0	-2.24	-1.44	
Ranbp3l	0	-2.18	-1.9	
Wdr49	0	-2.11	-0.93	
Ly6gef	0	-1.86	-1.72	
Lrrc43	0	-1.68	-1.49	
Gpr17	0	-1.52	-1.18	
Gli1	0	-1.44	-1.24	
Mob3b	0	-1.32	-1.24	
Hoxd1	0	-1.31	-0.87	
Rgs22	0	-1.28	-0.84	
Gdf7	0	-1.27	-0.99	
Cep72	0	-1.2	-0.75	
Vwa3a	0	-1.2	-0.86	
Dynlrb2	0	-1.2	-0.98	
Serp1b1	0	-1.19	-1	
Opn4	0	-1.17	-0.78	
Cd180	0	-1.17	-0.85	
Crb1	0	-1.12	-0.37	
Mxl1	0	-1.12	-0.98	
Fgfr2	0	-1.11	-0.87	
Dlec1	0	-1.1	-0.61	
Lrrc23	0	-1.08	-0.78	
Myh6	0	-1.06	-0.78	
Pls1	0	-1.05	-0.73	
Neil2	0	-1.05	-0.29	
Calr4	0	-1.04	-0.79	
Efs	0	-1.03	-0.87	
Adamts6	0	-1.03	-0.67	
Hhip	0	-1.02	-0.84	

D

Name	sham	SCI	CSCI	P
Gm6408	0	-1.63	-1.3	
Slc26a9	0	-3.9	0.009	
Olf1393	0	-3.4	-0.68	
Lrrc27	0	-3.04	-1.97	
Sis	0	-2.82	-1.26	
Vmn14	0	-2.65	0.032	
Ctcf1	0	-2.54	0.263	
Klf14	0	-2.47	-0.77	
Esco2	0	-2.45	-1.34	
Olf1545	0	-2.38	0.12	
Gm47283	0	-2.31	-0.26	
Gm40460	0	-2.31	-0.71	
Wdr86	0	-2.28	-0.83	
Esrp1	0	-2.21	-0.51	
E2f8	0	-2.2	-1.93	
Oard1	0	-2.04	-2.05	
Emilin3	0	-2	1.398	
Tulp1	0	-1.91	-0.52	
Ccdc153	0	-1.9	-1.44	
Lmtd1	0	-1.89	-1.28	
Iqca	0	-1.89	-1	
Pitx1	0	-1.88	-1.59	
Tmem212	0	-1.87	-1.08	
Mc5r	0	-1.85	-1.28	
Smim5	0	-1.84	-1.27	
D6Erd527e	0	-1.84	0.325	
Ccdc146	0	-1.81	-0.66	
Colea6	0	-1.81	-0.06	
Nme9	0	-1.74	-1.43	
Fam166b	0	-1.72	-1.38	
Ildr1	0	-1.71	-0.99	
Adgrf4	0	-1.67	-0.18	
Lgr6	0	-1.66	-1.49	
BC024139	0	-1.65	-1.22	
Clqmf3	0	-1.62	-1.38	
Acp4	0	-1.61	0.21	
Dnah8	0	-1.6	-0.66	
Accs1	0	-1.6	1.376	
Stpg1	0	-1.59	-1.08	
Dnah11	0	-1.57	-0.7	
Ninj2	0	-1.57	-1.23	
Slc27a5	0	-1.55	-0.08	
Tex35	0	-1.54	0.708	
Rad9a	0	-1.53	1.005	
Fscn2	0	-1.52	1.093	
Ttc16	0	-1.52	-1.01	
Mom5	0	-1.47	-0.28	
Fmpd2	0	-1.47	-0.64	
Col24a1	0	-1.46	-0.24	
Lrit3	0	-1.43	0.398	
Atp10b	0	-1.43	-1.11	
Sctr	0	-1.4	-0.55	
Cfap70	0	-1.38	-0.41	
Vwa3b	0	-1.38	-0.59	
Cdhr3	0	-1.37	-0.64	
Siglech	0	-1.35	-1	
Angptl1	0	-1.34	-1.49	
Kctd14	0	-1.33	-0.79	
Abcg5	0	-1.33	1.534	
Ing4	0	-1.31	-0.23	
Gm10775	0	-1.29	-0.07	
Mpp4	0	-1.29	0.129	
Mcm10	0	-1.27	0.212	
Neu4	0	-1.26	-1.14	
Aip1	0	-1.25	1.265	
Olfml1	0	-1.24	-1.02	
Cubn	0	-1.24	-0.12	
Barx2	0	-1.23	-0.31	
Slc34a3	0	-1.19	-0.83	
Tmem210	0	-1.17	-0	
Adamts19	0	-1.16	-0.43	
Cavin4	0	-1.16	-0.7	
Coll1a1	0	-1.13	-0.26	
H2-B1	0	-1.13	-0.45	
Nudh8	0	-1.12	-0.32	
Chrd	0	-1.12	-0.41	
Cfap44	0	-1.12	-0.1	
Cascl	0	-1.1	-0.24	
Gipr	0	-1.1	-0.65	
Ccdc162	0	-1.09	-0.56	
Tnfrsf4	0	-1.09	-0.41	
Pesk4	0	-1.08	-0.41	
Fxyd2	0	-1.05	-0.57	
Kif20b	0	-1.05	-0.58	
Pld6	0	-1.04	-0.44	
Entpd4b	0	-1.03	-0	
Coll1a2	0	-1.03	-0.47	
Riad1	0	-1.02	-0.43	
Ager	0	-1.01	-0.17	
Catsperd	0	-1.01	-0.26	
Rxfp1	0	-1.01	-0.48	
Smc1b	0	-1	0.496	
F2r13	0	-1	-0.2	
Poln	0	-1	-0.24	

DOWN

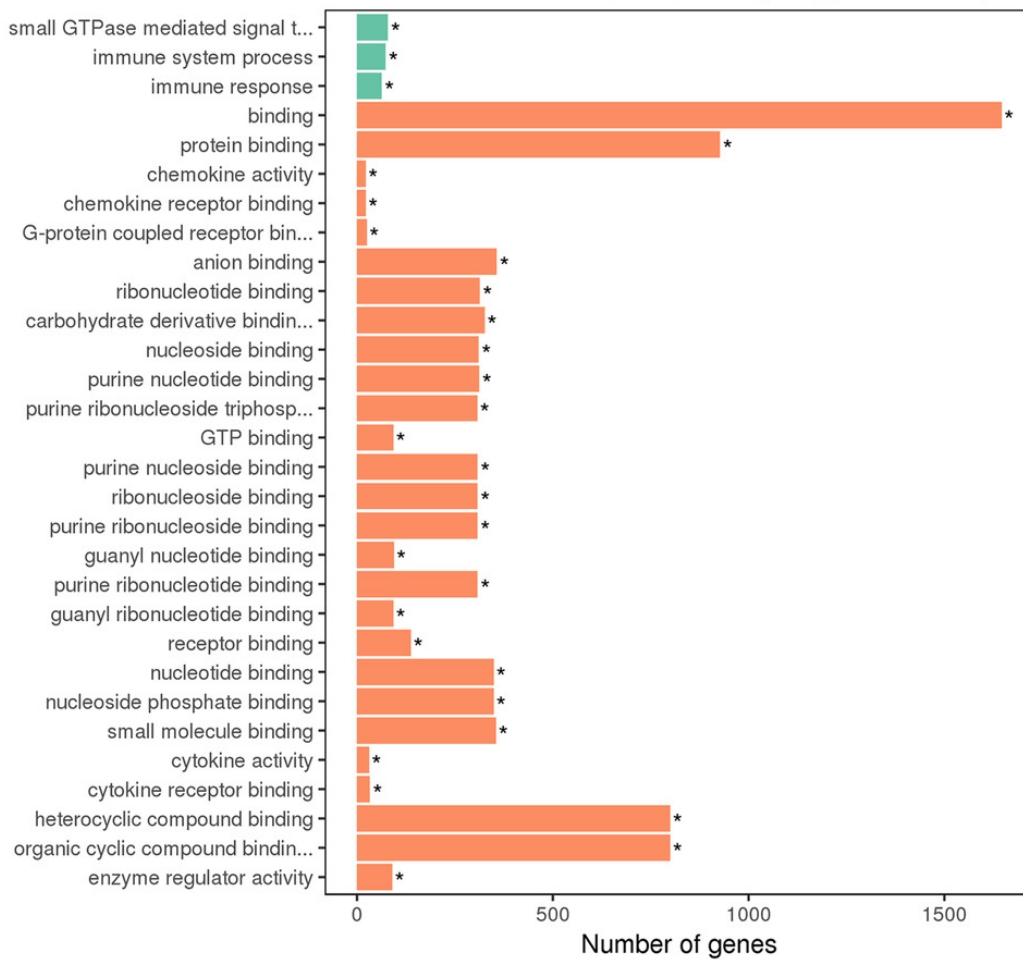
UP

Figure 6

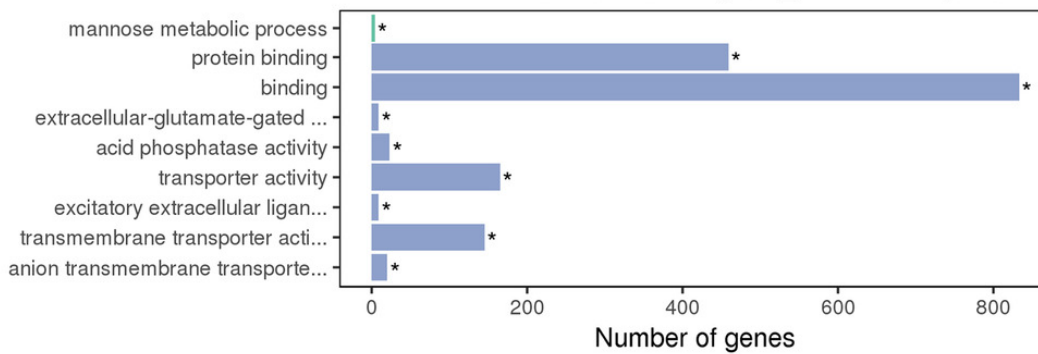
Figure 6 GO enrichment analysis of DEGs

DEGs were implemented by the Goseq R package, in which gene length bias was corrected. GO terms with corrected P value ≤ 0.05 were considered significantly enriched by DEGs. The asterisk (*) represent significant enrichment terms ($P \leq 0.05$). A: GO analysis of upregulated DEGs in SCI_C vs sham group; B: GO analysis of downregulated DEGs in SCI_C vs sham group; C: GO analysis of downregulated DEGs in SCI_P vs SCI_C group.

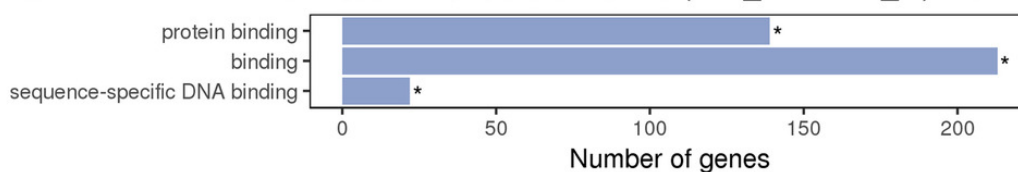
A Enriched GO Terms (SCI_C vs sham) **UP**



B Enriched GO Terms (SCI_C vs sham) **DOWN**



C The Most Enriched GO Terms (SCI_P vs SCI_C) **DOWN**



type ■ biological_process ■ cellular_component ■ molecular_function

Figure 7

Figure 7 KEGG enrichment analyses of DEGs

KOBAS software was used to test the statistical enrichment of DEGs in KEGG pathways. In this figure, KEGG enrichment is measured by Rich factor, Qvalue and the number of genes enriched in the related pathway. Rich factor refers to the ratio of the number of differentiated genes (sample number) enriched in the pathway to the number of annotated genes (background number). The larger the Rich factor, the greater the degree of enrichment. Qvalue is the Pvalue after multiple hypothesis test correction. The range of Qvalue is between 0 and 1. The closer the Qvalue is to 0, the more significant the enrichment is. The KEGG pathways were shown in A: upregulated DEGs (SCI_C vs sham); B: downregulated DEGs; C: upregulated DEGs (SCI_P vs SCP_C); D: downregulated DEGs (SCI_C vs sham).

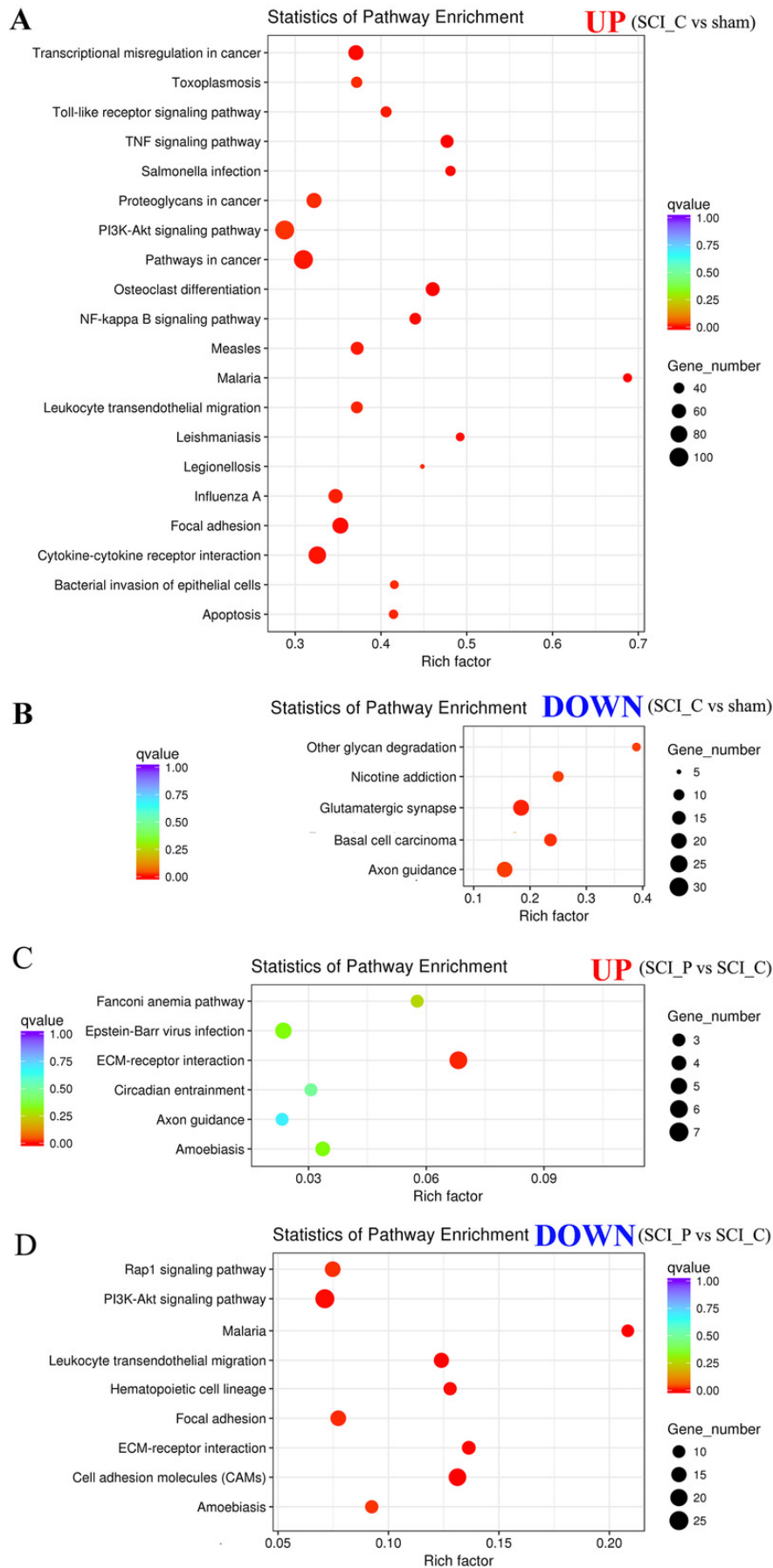


Table 1 (on next page)

Table 1 PCR primers used in the study

1 **Table 1 Real-time PCR primers used in the study**

2

Gene	Forward primer 5' - 3'	Reverse primer 5' - 3'
Itga1	TCAGTGGAGAGCAGATCGGA	CCTCGTCTGATTCACAGCGT
lamb1	TGCCTTTTCTCCCCGCTACC	CCATGTCCAGTCCTCGCAGA
Cldn5	TTCTATGATCCGACGGTGCC	CTTGACCGGGAAGCTGAACT
CD34	ACCACAGACTTCCCCAACTG	CATATGGCTCGGTGGGTGAT
lama2	GCATTAGTGAGCCGCCCTAT	TCTTTCAGGTCTCGTGTGGC
Esam	AGACTCTGGGACTTACCGCT	GGTCACATTGGTCCCGACAT
Setdb2	CCACAAATGGAGATCATAACCT	GCAGTGGGGCTTCCTTTTTC
Agri	CTCTGCCACTGGAACACAGA	GGAAAAGCAGCACCGCAAAG
Ccnt2	AGCAAGGATTTGGCACAGAC	CTCTAGGGTAACCGTGGGGT
beta-actin	AGAAGCTGTGCTATGTTGCTCTA	ACCCAAGAAGGAAGGCTGGAAAA

Table 2 (on next page)

Table 2 Summary of sequence assembly after Illumina sequencing

Sham: Sham_1, Sham_2, Sham_3; SCI (solvent control): SCI_C1, SCI_C2, SCI_C3; SCI

(probenecid): SCI_P1, SCI_P2, SCI_P3; Q20: The percentage of bases with a Phred value > 20;

Q30: The percentage of bases with a Phred value > 30.

1 **Table 2 Summary of sequence assembly after Illumina sequencing**

2

Sample name	Raw reads	Clean reads	clean bases	Error rate (%)	Q20 (%)	Q30 (%)	GC content (%)
Sham_1	56509230	55796658	8.37G	0.03	97.73	93.95	51.23
Sham_2	48848744	48226002	7.23G	0.03	97.6	93.67	51.71
Sham_3	58228350	57459748	8.62G	0.03	97.67	93.78	51.42
SCI_C1	58862872	58126844	8.72G	0.03	97.88	94.31	51.39
SCI_C2	56980070	56166058	8.42G	0.03	97.74	94.03	51.42
SCI_C3	59804518	58798224	8.82G	0.03	97.63	93.74	51.02
SCI_P1	54853344	53996254	8.1G	0.03	97.72	93.91	50.93
SCI_P2	56322736	55540308	8.33G	0.03	97.87	94.27	50.94
SCI_P3	61037096	60037772	9.01G	0.03	97.71	93.89	50.92

3 Sham: Sham_1, Sham_2, Sham_3; SCI (solvent control): SCI_C1, SCI_C2, SCI_C3; SCI (probenecid): SCI_P1, SCI_P2,

4 SCI_P3;

5 Q20: The percentage of bases with a Phred value > 20;

6 Q30: The percentage of bases with a Phred value > 30.

7